



# Potential and limitations of $^{13}\text{C}$ CP/MAS NMR spectroscopy to determine the lignin content of lignocellulosic feedstock

Daniel F. Cipriano<sup>a,\*</sup>, Luiz S. Chinelatto Jr.<sup>b</sup>, Sandra A. Nascimento<sup>c</sup>, Camila A. Rezende<sup>c</sup>,  
Sonia M.C. de Menezes<sup>b</sup>, Jair C.C. Freitas<sup>a</sup>

<sup>a</sup> Laboratory of Carbon and Ceramic Materials, Department of Physics, Federal University of Espírito Santo (UFES), 29075-910, Vitória, ES, Brazil

<sup>b</sup> PETROBRAS/CENPES, Av. Horácio Macedo, 950, Cidade Universitária, 21941-915, Rio de Janeiro, RJ, Brazil

<sup>c</sup> Institute of Chemistry, University of Campinas (UNICAMP), PO Box 6154, 13083-970, Campinas, SP, Brazil

## ARTICLE INFO

### Keywords:

Lignocellulosic biomass  
Lignin content  
Solid-state  $^{13}\text{C}$  NMR  
Acid hydrolysis

## ABSTRACT

Nuclear magnetic resonance (NMR) spectroscopy has been applied worldwide to study the chemical composition of lignocellulosic biomass and to analyse changes resulting from the chemical processing of these materials. In this work, solid-state  $^{13}\text{C}$  NMR was used to study the lignin contents of a large set of lignocellulosic materials derived from various Brazilian plant species. To determine the lignin content by NMR, the integrated intensity of the deconvoluted signal due to methoxyl groups in the  $^{13}\text{C}$  NMR spectra was used to obtain a calibration curve using mixtures of cellulose and lignin standards. The lignin contents obtained by NMR were, in general, in good agreement with the results obtained by methods based on acid hydrolysis (AH). For some samples, the NMR results showed that the AH methods were ineffective for the complete carbohydrate hydrolysis, indicating that the NMR-derived values represented more reliable estimates of the lignin contents in these cases.

## 1. Introduction

Lignocellulosic biomass is an important source for the production of biofuels and biomaterials aiming at different technological applications [1–3]. There are several examples of lignocellulosic feedstocks, such as forest biomass, agricultural residues, marine algae and herbaceous grasses, which can be used to replace non-renewable energy sources, such as oil and coal [4,5]. However, the application of lignocellulosic components faces some limitations that need to be overcome in order to reduce the production cost of the final products. These include the necessity of breaking down the intricate network that constitutes the lignocellulosic structure, which can involve chemical, mechanical or biological methods, among others [6,7].

Plant cell wall in lignocellulosic biomass has three main components: cellulose, hemicellulose and lignin. These organic components form a recalcitrant structure responsible for the plant mechanical strength and that allows water and nutrient transportation through the plant [8,9]. Cellulose is made up from D-glucose chains organised in a linear structure known as cellulose microfibril. In turn, hemicellulose – which is considered as the connection between cellulose and lignin – is amorphous and formed by different monosaccharides, linked to cellulose

microfibrils by hydrogen bonds [10,11].

Lignin is a three-dimensional, predominantly aromatic polymer, with a structure mainly composed of three different phenylpropane units: *p*-hydroxyphenyl (H), guaiacyl (G), and syringyl (S). The difference between these units is the occurrence of methoxyl groups attached to carbons 3 and 5 of the aromatic ring [12]. Lignin is responsible for binding the cells and supporting the cellulosic network [8]; it has been widely used as a fuel in paper industry and biorefineries, but there are also several applications as a polymer precursor due to its thermoplastic properties and high percentage of hydroxyl groups [13,14]. Lignin can also be used as an inexpensive feedstock to produce chemicals and as an additive in materials for mechanical reinforcement, improvement of antioxidant and antimicrobial activity, ultraviolet protection and in biomedical applications [15,16].

In the lignocellulosic framework, the carbohydrate fractions are embedded into a lignin-rich matrix that is the principal barrier to degradation of the polymeric structure and its conversion into fuels and chemical feedstocks [4,17]. Several methods have been successfully applied for the separation and utilization of the lignocellulosic components, including mechanical pretreatments, chemical and/or biochemical reactions [7,18]. Knowledge about lignin and carbohydrate contents

\* Corresponding author.

E-mail address: [daniel.cipriano@ufes.br](mailto:daniel.cipriano@ufes.br) (D.F. Cipriano).

<https://doi.org/10.1016/j.biombioe.2020.105792>

Received 20 May 2019; Received in revised form 3 August 2020; Accepted 14 September 2020

Available online 30 September 2020

0961-9534/© 2020 Elsevier Ltd. All rights reserved.

of lignocellulosic materials is of chief importance to monitor the changes in these fractions during the course of the used treatments [19,20]. Most analytical methods for the determination of lignin and carbohydrate contents are destructive, time-consuming, demand high amounts of material and generate a lot of chemical residues [21]. Consequently, it is highly desirable to develop simple and quick spectroscopic-based methods for the determination of these contents, among which solid-state  $^{13}\text{C}$  nuclear magnetic resonance (NMR) appears as one of the most attractive alternatives.

NMR has been worldwide used to study the chemical composition of lignocellulosic biomass and to analyse changes resulting from the isolation processes of lignocellulosic components or from several types of thermal/chemical processes [22–24]. However, some problems can hamper quantitative analyses in lignocellulosic materials by solid-state NMR, including the overlapping of signals, the long spin-lattice relaxation of  $^{13}\text{C}$  nuclei in quantitative direct polarization (DP) experiments and the non-homogeneous transfer of polarization in  $^1\text{H}$ - $^{13}\text{C}$  cross-polarization experiments (CP) [25]. Even so, some studies have been able to show that it is possible to use solid state NMR as a fast method to study the lignin contents in biomass from the analysis of the intensity of lignin signals in the spectrum [26–29].

In 1984, Haw et al. employed a combination of CP with magic-angle spinning (MAS) in  $^{13}\text{C}$  NMR spectroscopy to study the lignin content of wood samples, by assuming an average molecular formula for conifer lignin [28]. More recently, Sievers et al. (2009) used linear combinations of solid-state  $^{13}\text{C}$  NMR spectra to determine the lignin and carbohydrate contents of residues from acid hydrolysis of wood. Other authors used a calibration curve constructed from the intensity of the aromatic signals in the solid-state  $^{13}\text{C}$  NMR spectra of pure lignin to determine lignin contents in biologically modified samples [26]. In a related work, Gao et al. (2015) proposed a similar approach to predict the lignin content of different kinds of biomass materials, but also taking advantage of the use of an internal intensity standard.

Whereas these recent efforts demonstrate the potential of the use of solid-state NMR for quantitative analyses of lignin contents in lignocellulosic materials, some points still remain open. For instance, the choice of an adequate lignin standard, since lignin chemical composition and structure can vary among distinct biomass materials so that there is no universal standard for this lignocellulosic component [24,30]. Also, the number of different types of lignocellulosic materials encompassed in these studies is quite limited.

In this work,  $^{13}\text{C}$  CP/MAS NMR spectra were used for the assessment of the lignin contents in a wide variety of biomass materials, including wood samples, fruit shells and lignocellulosic residues in a total of 41 analysed samples. The NMR-derived lignin contents were compared to the results obtained with one of the standard methods of lignin quantification based on acid hydrolysis (AH) of carbohydrates, also known as Klason method [31]. With this approach, it was possible to ascertain the potential and limitations of solid-state NMR methods for lignin quantification. In some cases, the NMR method was more appropriate than the laborious AH-based methods, since the solid residue obtained by the latter (which is assumed to represent insoluble lignin and ash in the material) clearly contained significant amounts of residual carbohydrates, as revealed by  $^{13}\text{C}$  CP/MAS NMR spectroscopy. Besides that, the differences in the lignin chemical structure of different lignocellulosic materials played an important role in the effectiveness of the NMR quantification method. The proposed approach is particularly promising as a fast and non-destructive method to assess the variation of lignin contents in chemically modified lignocellulosic materials, thus allowing the monitoring of the changes brought about by chemical/biochemical treatments performed with biomass feedstocks.

## 2. Materials and methods

### 2.1. Materials

The standard cellulose sample used in the NMR analyses was provided by Sigma-Aldrich (reference 22183). The standard lignin sample was obtained by the Kraft method from eucalyptus wood, and kindly provided by Fibria (Aracruz, ES, Brazil). This standard lignin was chosen due to its high purity, as revealed by  $^{13}\text{C}$  CP/MAS NMR spectroscopy, thermogravimetry (TG) and energy dispersive X-ray spectroscopy (EDX) analyses conducted for a set of lignin samples (including the eucalyptus lignin sample and two commercial ones). The standard lignin exhibited the lowest ash content (ca. 2%) and the best signal-to-noise (S/N) ratio in the corresponding  $^{13}\text{C}$  CP/MAS NMR spectrum. On the other hand, the commercial lignin samples presented higher ash contents (ca. 18–20%) and significant amounts of sulphur in their composition, as observed by EDX analyses. Thus, the better S/N ratio obtained in the  $^{13}\text{C}$  NMR spectrum of the standard lignin sample is probably due to its lower ash content, since only the organic compounds contribute to the recorded  $^{13}\text{C}$  NMR spectra. The cellulose and lignin standard samples were then used to prepare eleven mixtures in the following cellulose: lignin mass ratios: 90:10, 85:15, 80:20; 75:25; 70:30, 67:33, 60:40; 50:50; 40:60; 33:67; 15:85.

As for the biomass materials, 20 raw lignocellulosic samples from several plant sources were selected, as detailed in Table 1. The two samples named lignocel (LC) and Monterey pine whole (MPW) (*Pinus radiata*) are commercial samples of softwood provided by J. Rettenmaier & Söhne and by Sigma-Aldrich, respectively. The other samples described in Table 1 are agricultural wastes abundant in Brazil, including sugarcane bagasse (*Saccharum spp.*) and different species of palms used for oil extraction. Sugarcane bagasse 1 (SB1) and sugarcane bagasse 2 (SB2) were kindly provided by the sugarcane mill São

**Table 1**

Lignin contents determined by NMR and AH methods for the raw lignocellulosic materials, together with the values of the ratio  $r\text{SG}$  obtained by  $^{13}\text{C}$  CP/MAS NMR.

Sample	Lignin Content (%)		$r\text{SG}$ (=I153/I148+I145)
	NMR	AH	
Sugarcane bagasse 1 (SB1)	19 (3) <sup>†</sup>	22	0.60 <sup>††</sup>
Sugarcane bagasse 2 (SB2)	21 (3)	23	0.64
Sugarcane bagasse 3 (SB3)	23 (4)	19	0.59
Monterey pine whole (MPW)	26 (4)	27	0.17
Lignocel 1 (LC1)	29 (4)	32	0.42
Lignocel 2 (LC2)	28 (4)	29	0.18
Açaí stone (AS)	21 (4)	21*	2.11
Endocarp of babassu coconut 1 (EBC1)	38 (3)	38*	1.01
Endocarp of babassu coconut 2 (EBC2)	36 (4)	44*	1.14
Oil palm leaf (OPL)	27 (4)	26	2.81
Oil palm empty fruit bunch (OPEB)	26 (4)	20	2.00
Oil palm fruit bunch (OPFB)	30 (4)	35*	2.15
Oil palm sterilized empty fruit bunch (OPSB)	30 (3)	24	1.63
Oil palm bunch straw (OPBS)	31 (4)	34	1.31
Oil palm rachis (OPR)	29 (4)	30	1.79
Palm kernel shell 1 (PKS1)	33 (4)	59*	1.32
Palm kernel shell 2 (PKS2)	40 (4)	65*	1.45
Macaúba empty fruit bunch (MB)	28 (3)	34	0.61
Macaúba kernel shell 1 (MKS1)	26 (3)	67*	0.57
Macaúba kernel shell 2 (MKS2)	28 (3)	62*	0.61

<sup>†</sup>The numbers between parentheses are the uncertainties in the last digit.

<sup>††</sup>The parameter  $r\text{SG}$  is defined as the ratio between the intensity of the  $^{13}\text{C}$  NMR signal at 153 ppm (I153) and the sum of the intensities of the signals at 145 and 148 ppm (I148+I145).

\*Samples for which carbohydrate signals were detected in the  $^{13}\text{C}$  CP/MAS NMR spectra of the corresponding AH residues.

Martinho (Pradópolis, SP, Brazil). Sugarcane bagasse 3 (SB3) was kindly provided by the sugarcane mill Cruz Alta (Guarani, SP, Brazil). Açai stone (AS) (*Euterpe oleracea*) is a processing residue that was collected at several açai stores in the metropolitan region of Belém, PA, Brazil. Endocarp of babassu coconut 1 (EBC1) (*Orbignya speciosa*) was provided by local producers from the municipality of Açailândia, MA, Brazil. Endocarp of babassu coconut 2 (EBC2) was kindly provided by the babassu oil and activated carbon industry TOBASA Bioindustrial de Babaçu S.A. (Tocantinópolis, TO, Brazil). Oil palm leaf (OPL) (*Elaeis guineensis*), oil palm empty fruit bunch (OPEB), oil palm fruit bunch (OPFB), oil palm sterilized empty fruit bunch (OPSB), oil palm bunch straw (OPBS), oil palm rachis (OPR), palm kernel shell 1 (PKS1) and palm kernel shell 2 (PKS2) are by-product streams of palm oil production process and they were kindly provided by Companhia Refinadora da Amazônia - Agropalma Group (Belém, PA, Brazil). Macaúba empty fruit bunch (MB) (*Acrocomia aculeata*), macaúba kernel shell 1 (MKS1) and macaúba kernel shell 2 (MKS2) were obtained from the cooperative Cooper Riachão (Montes Claros, MG, Brazil).

Another group of materials analysed here comprises samples from three different kinds of biomass sources (sugarcane bagasse, elephant grass and eucalyptus bark), which underwent distinct chemical treatments, as described in Table 2. Sugarcane bagasse (SB) (*Saccharum spp.*)

**Table 2**

Lignin contents determined by NMR and AH methods for the chemically treated lignocellulosic materials, together with the values of the ratio  $rSG$  obtained by  $^{13}C$  CP/MAS NMR.

Sample	Lignin Content (%)		$rSG$ (=I153/I148+I145)
	NMR	AH	
Sugarcane bagasse (SB)	22 (4) <sup>†</sup>	22.2 (1)	0.99 <sup>††</sup>
SB after 1% H <sub>2</sub> SO <sub>4</sub> (SBH1)	23 (4)	29.5 (6)	0.50
SBH1 after 0.25% NaOH (SBN0.25)	21 (4)	25.2 (3)	0.45
SBH1 after 0.5% NaOH (SBN0.5)	17 (3)	23 (7)	0.97
SBH1 after 1% NaOH (SBN1)	11 (3)	11.0 (9)	n.d. <sup>†††</sup>
SBH1 after 2% NaOH (SBN2)	12 (3)	9.5 (5)	n.d.
SBH1 after 3% NaOH (SBN3)	9 (3)	9.5 (5)	n.d.
SBH1 after 4% NaOH (SBN4)	7 (3)	9.3 (4)	n.d.
Elephant grass (EG)	19 (3)	25 (2)	0.69
EG after 5% NaOH (EGN5)	12 (3)	13.7 (4)	n.d.
EGN5 after 4% of NaOH and 7 % of H <sub>2</sub> O <sub>2</sub> (EGN4)	8 (3)	9.9 (2)	n.d.
Eucalyptus bark (EB)	24 (4)	23	2.59
EB after 1% NaOH for 40 min (EBN1_40)	25 (4)	21.8	2.77
EB after 5% NaOH for 40 min (EBN5_40)	25 (4)	20.3	3.63
EB after 1% NaOH for 80 min (EBN1_80)	23 (4)	23.4	2.94
EB after 5% NaOH for 80 min (EBN5_80)	27 (4)	19.9	3.65
EB after 1% H <sub>2</sub> SO <sub>4</sub> and 1% NaOH for 40 min (EBH1N1_40)	27 (4)	24.3	2.87
EB after 1% H <sub>2</sub> SO <sub>4</sub> and 5% NaOH for 40 min (EBH1N5_40)	23 (4)	21.3	3.09
EB after 1% H <sub>2</sub> SO <sub>4</sub> and 1% NaOH for 80 min (EBH1N1_80)	26 (4)	25.2	1.98
EB after 1% H <sub>2</sub> SO <sub>4</sub> and 5% NaOH for 80 min (EBH1N5_80)	22 (4)	23.6	2.35
EB after 0.5% H <sub>2</sub> SO <sub>4</sub> and 3% NaOH for 60 min (EBH0.5N3_60)	23 (4)	23.5	3.20

<sup>†</sup>The numbers between parentheses are the uncertainties in the last digit.

<sup>††</sup>The parameter  $rSG$  is defined as the ratio between the intensity of the  $^{13}C$  NMR signal at 153 ppm (I153) and the sum of the intensities of the signals at 145 and 148 ppm (I148+I145).

<sup>†††</sup>n.d. = not determined; for these samples, it was not possible to obtain reliable values of the deconvoluted intensities in the aromatic spectral region, due to the low intensity of the corresponding  $^{13}C$  NMR spectra in that region, associated with the reduced amounts of lignin.

was kindly provided by the Cosan Group (Ibaté, SP, Brazil) and used as received, after drying in a convection oven at 60 °C for 24 h. Typically, the sugarcane stalks were harvested 12 months after planting and the possible varieties of sugarcane contained in the SB sample are SP81-3250, RB85-5156, RB86-7515 and/or SP83-2847. The samples were passed through a 9.8 mm sieve, treated with diluted H<sub>2</sub>SO<sub>4</sub> (1% v/v) and then submitted to alkali treatments using different concentrations of NaOH (0.25, 0.5, 1, 2, 3, 4 and 5% w/w). More details about the treatments carried out can be found in a previous work [19].

Elephant grass (EG) (*Pennisetum purpureum*) leaves were kindly provided by the Institute of Animal Science (Instituto de Zootecnia, Nova Odessa, SP, Brazil) from plants harvested 12 months after planting. This sample was dried at 60 °C for 24 h and knife milled (SL-31 SOLAB) until passing through a 2 mm sieve. Next, the sample was treated with NaOH (5% w/w) and the resulting product was named sample EGN5. This material was then submitted to two bleaching steps with a 1:1 solution of NaOH (4% w/w) and H<sub>2</sub>O<sub>2</sub> (7% v/v), giving rise to sample EGN4. More details about the performed treatments can be found elsewhere [32].

Eucalyptus bark (EB) samples were obtained from *Eucalyptus grandis* clones and were kindly donated by Suzano Papel e Celulose (Suzano, SP, Brazil). The EB samples were dried at 60 °C for 24 h and knife milled (SL-31 SOLAB) until passing through a 2 mm sieve; next, the samples were treated with different concentrations of H<sub>2</sub>SO<sub>4</sub> (0.5 and 1% v/v) and NaOH (1, 3 and 5% w/w) during different treatment times, as shown in Table 2.

## 2.2. Determination of the lignin contents by wet chemical methods

The acid insoluble lignin contents of the natural biomass materials presented in Table 1 were determined using the AH method [31]. Briefly, milled and dried samples were extracted with acetone, followed by hydrolysis with a 72% (w/w) H<sub>2</sub>SO<sub>4</sub> solution at 30 °C for 1 h; the hydrolysate was diluted in water and taken to a reactor where it remained at 120 °C for 1 h. The solid residue was separated by filtration and, after correction for moisture and ash contents (determined using TG), the solid material was assumed to represent the lignin content of the samples ("Klason lignin").

For the samples listed in Table 2, the total lignin (soluble and insoluble) content is reported. Insoluble lignin was determined as described above and in other reports in the literature [19,32], while acid soluble lignin was determined using UV-Vis spectroscopy to analyse the liquor resulting from the AH step [30].

## 2.3. Solid-state NMR analysis

NMR spectra were recorded in a Varian/Agilent 400 MHz NMR spectrometer operating at 9.4 T (NMR frequency of 100.5 MHz for  $^{13}C$ ), using a solid-state NMR probe equipped with zirconia rotors (4 mm diameter). Prior to the analyses, all samples passed through a 60 mesh sieve and were then packed into the rotors.

All the  $^{13}C$  CP/MAS NMR spectra were recorded with samples at room temperature. A ramp CP pulse sequence was used, with high-power  $^1H$  decoupling (SPINAL method) during acquisition of the free induction decay (FID). Other acquisition parameters were: 10 kHz of MAS rate; 3.6  $\mu s$  of  $^1H$  pulse duration ( $\pi/2$  pulse); 5 s of recycle delays; 20.48 ms of acquisition time; 50 kHz of spectral width; 1500 recorded transients and 1 ms of contact time (chosen after careful optimization in variable contact time experiments). The spectra were obtained by Fourier transform of the FIDs and were externally referenced by tetramethylsilane (TMS), using hexamethylbenzene (HMB) as a secondary reference (17.3 ppm for the methyl groups).

The  $^{13}C$  DP/MAS NMR spectra were recorded for three selected samples: standard lignin, sugarcane bagasse and palm kernel shell. The  $^{13}C$  pulse duration was 4.3  $\mu s$  ( $\pi/2$  pulse), with a 20.48 ms acquisition time, around 2000 recorded transients and a 100 s recycle delay. The

pulse sequence included also a pair of  $\pi$  pulses applied just after the  $\pi/2$  pulse, in order to avoid probe background signals [33].

All recorded spectra were deconvoluted using a combination of Gaussian and Lorentzian lines in the program ACD/NMR Processor Academic Edition [34].

#### 2.4. Determination of the lignin contents by solid-state $^{13}\text{C}$ NMR

After careful spectral deconvolution of all  $^{13}\text{C}$  CP/MAS NMR spectra, the spectral region associated with lignin methoxyl ( $\text{OCH}_3$ ) groups was chosen for the assessment of the lignin content in the material. As an alternative procedure, the intensity obtained by direct integration of the methoxyl signal was also calculated for a selected group of cellulose-lignin mixtures and for the biomass materials analysed in this work, as detailed in the Supplementary Material. Though it is quite well known that lignin derived from different types of plants exhibits distinct relative amounts of methoxyl groups [35,36], the analysis of the lignin contents for the materials described in this work did not seem to be decisively influenced by this choice. Alternative calibration procedures using the spectral intensity due to aromatic carbons – similarly to the methods described by Fu et al. (2015) and Gao et al. (2015) – were also tested, but the obtained results were not improved in comparison with the method based on the spectral intensity due to methoxyl groups, as detailed in Section 3.1. The signal assigned to methoxyl groups (at ca. 56.3 ppm) as the indicator of lignin contents was therefore preferred due to its larger S/N ratio as compared to the signals due to aromatic carbons. This allowed the NMR experiments to be carried out in moderate experimental time ( $\sim 2$  h), in contrast to previous works, where 24 h were necessary for each spectrum [26,29].

To determine the lignin contents in the samples, a calibration curve was obtained with  $^{13}\text{C}$  CP/MAS NMR spectra recorded for the cellulose/lignin mixtures. The integrated intensity of the signal due to methoxyl groups (obtained by spectral deconvolution) was plotted as a function of the lignin mass in the mixture.  $^{13}\text{C}$  CP/MAS NMR spectra were also recorded for the samples of lignocellulosic materials under the same experimental conditions and the lignin content was determined using the calibration curve and considering the dry sample weight in the rotor. For each lignocellulosic material analysed, the mass of lignin in the sample was calculated using the calibration curve and the deconvoluted intensity of the methoxyl signal; then, the lignin content was obtained by the ratio between the calculated lignin mass and the mass of the dry sample in the rotor. The uncertainty in the lignin contents was estimated by propagation of uncertainties obtained by repeating the whole procedure for triplicates taken from the same standard lignin sample and also by considering the error bars associated with the equation corresponding to the calibration curve.

### 3. Results and discussion

#### 3.1. Determination of the lignin contents of lignocellulosic materials from various sources using solid-state $^{13}\text{C}$ NMR

$^{13}\text{C}$  CP/MAS NMR spectra obtained for pure lignin, for pure cellulose, for a 50:50 cellulose: lignin mixture and for sugarcane bagasse (sample SB1, as a representative lignocellulosic material chosen among the analysed samples) are shown in Fig. 1a, 1b, 1c and 1d, respectively. In the SB1 spectrum (Fig. 1d), the signals associated with the three main components of the lignocellulosic structure – i.e., lignin (L), cellulose (C) and hemicellulose (H) – are identified [28,37]. The most intense peaks in the spectra shown in Fig. 1c and d are associated with the carbohydrates, containing superimposed contributions of carbon atoms from cellulose and hemicellulose. This overlap imposes barriers to the proper separation of the information about these two components in this type of spectra. With respect to lignin, the signals due to methoxyl and aromatic carbons are detected in spectral regions more easily separated from the carbohydrate signals. These lignin signals are thus potentially useful for

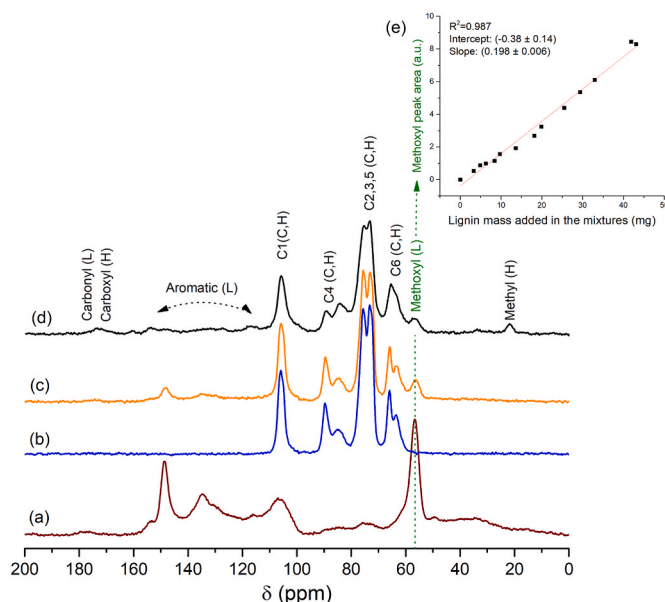


**Fig. 1.**  $^{13}\text{C}$  CP/MAS NMR spectra of (a) pure lignin, (b) pure cellulose, (c) 50:50 cellulose: lignin mixture and (d) sugarcane bagasse sample. The letters C, H and L indicate the signals associated with cellulose, hemicellulose and lignin, respectively. The main carbohydrate signals are labelled according to the common terminology used to identify the carbon atoms in the anhydroglucose repeating unit in cellulose and hemicellulose. Part (e) shows the calibration curve correlating the lignin contents with the area of the signal due to methoxyl groups in the  $^{13}\text{C}$  NMR spectra, obtained by deconvolution of the spectra.

determining the lignin contents in biomass materials [26]; however, in the spectra obtained for lignocellulosic materials (as the one shown in Fig. 1d), the aromatic signals are weaker and poorly resolved compared to the signal due to methoxyl groups. Fig. 1a shows that the methoxyl signal (at ca. 56.3 ppm) is dominant in the  $^{13}\text{C}$  CP/MAS NMR spectrum of lignin and that it can be easily separated from the carbohydrate C6 peak by spectral deconvolution (as shown in the Supplementary Material); this suggests that the methoxyl signal may be an interesting choice for the quantification of lignin content in lignocellulosic materials. On the other hand, the fact that lignin from different plant sources presents distinct amounts of methoxyl groups in their molecular structure [38, 39] poses some questions on the accuracy and limits of validity of this quantification method, as discussed later.

To construct a calibration curve from the intensity of the signal due to methoxyl groups, the  $^{13}\text{C}$  CP/MAS NMR spectra of mixtures of cellulose and lignin (such as the one shown in Fig. 1c) were deconvoluted and the absolute integrated intensity (i.e., the non-normalized area of the peak used in the spectral deconvolution) of the signal at ca. 56.3 ppm was separately determined for each mixture. This area was correlated with the mass of lignin in each mixture, leading to the linear regression shown in Fig. 1e. Using this calibration curve, the lignin contents of a large set of different biomass materials were determined. These NMR lignin contents were then compared to the contents determined by the AH method, as shown in Tables 1 and 2. The corresponding results obtained using an alternative method of direct integration of a chemical shift window around the methoxyl peak (instead of spectral deconvolution) are also discussed in the Supplementary Material.

As it can be clearly seen in the comparison shown in Tables 1 and 2, the agreement between the NMR results and the AH method is quite good, with the exception of 5 samples in Table 1 (EBC2, PKS1, PKS2, MKS1 and MKS2); for these samples, the hydrolysis of the carbohydrates was not complete, as revealed by the  $^{13}\text{C}$  CP/MAS NMR spectra recorded for the AH residues. Excluding for the time being these outliers (which will be analysed in detail in Section 3.3), the AH lignin contents of all other natural samples are plotted as a function of the respective NMR

lignin contents in Fig. 2. The correlation between these values is remarkably good, with 11 of the 15 values agreeing within the uncertainty limits for the different analysed samples. Similar results were also obtained when a different NMR spectrometer (operating under another magnetic field) was used to record the NMR spectra, as described in the Supplementary Material, which illustrates the robustness of the developed quantification method and its general applicability using different instruments, when the appropriate calibration procedures are correctly implemented.

It is known that the methoxyl group occurrence in the lignin structure varies among different plants, for different parts of the plants and even for plants of the same variety but grown in different climatic and soil conditions [21]. Generally, guaiacyl units are predominant in lignin derived from softwood, whereas in hardwood both guaiacyl and syringyl units are present in similar amounts in the lignin structure. In grasses, the amount of p-hydroxyphenyl units may be slightly higher than in other plants [14,36].

Considering the occurrence of these lignin units in different amounts for distinct biomass materials, it is reasonable to conclude that any spectroscopic (e.g., NMR) method aimed at quantifying the lignin content in a given material will be more accurate if a lignin sample extracted from the same material is used as a reference standard. This approach was recently followed by Fu et al. (2015), who used the intensity of the aromatic signals in  $^{13}\text{C}$  NMR spectra as an indicator of the lignin content in kenaf-derived samples and took lignin derived from the same source as an intensity standard [26]. However, for a method widely applicable to different biomass materials, this approach has little practical use. Thus, the use of a common lignin standard sample is required, which undoubtedly limits the accuracy of the obtained lignin contents.

In a study of the chemical composition of biomass materials using near infrared spectroscopy, Sanderson et al. (1996) showed that it is possible to predict the lignin contents with acceptable accuracy using a calibration curve constructed from the analysis of a broad set of different samples. It was also noted in their work that, though this approach reduces the accuracy of the method, it allows the achievement of reasonable estimates of the lignin contents without the costs involved in the development of a specific calibration curve for each type of biomass material to be analysed [40].

Furthermore, it is important to observe that the comparison shown in Fig. 2 includes a large number of lignocellulosic materials from various plant sources (e.g., fruit shells, straw, wood, bagasse and others). There is no reason to suspect that the lignin chemical composition would be exactly the same in all samples of this group, and not even to assume that any of these lignin forms would be similar to the standard lignin sample

used to construct the NMR calibration curve. Therefore, the successful correlation shown in Fig. 2 illustrates the robustness of the quantification method based on the use of the intensity of the signal due to methoxyl groups in the  $^{13}\text{C}$  CP/MAS NMR spectra, at least for the purpose of estimating the lignin contents of different biomass materials with a tolerance of ca. 5% in comparison with the AH lignin contents.

It is also interesting to note that the use of a calibration curve constructed using a common lignin standard sample to assess the lignin contents of a diversified group of lignocellulosic materials is somewhat similar to assuming a single average molecular formula to describe the lignin composition in these materials. This approach has been used, for example, for the determination of the lignin contents in softwoods directly from the integration of  $^{13}\text{C}$  CP/MAS NMR spectra [28]. The problems and limitations with this type of assumption have been discussed for a long time and are in many cases unavoidable when spectroscopic methods are employed to quantify the carbohydrate and lignin contents in lignocellulosic materials [30,41]. However, the results presented in this work show that this approach can indeed be useful when quick (and not too accurate) estimates of the lignin contents of different biomass materials are desired.

The quantitative analyses of the lignin contents of the same biomass materials were also performed using the intensity of the signals due to aromatic carbons in the  $^{13}\text{C}$  CP/MAS NMR spectra, similarly to the method described by Fu et al. (2015) [26]. However, the agreement between the NMR-derived and the AH lignin contents, as presented in the Supplementary Material, was worse in this case, in comparison to the values obtained using the intensity of the signal due to methoxyl groups. The reason for this is probably related to the inferior S/N ratio of the aromatic signals, which are spread over a chemical shift range (~50 ppm) considerably larger than the one corresponding to the methoxyl signal (~10 ppm). Also, it is important to note that, similarly to what was discussed above for the methoxyl signal, the aromatic signals in the  $^{13}\text{C}$  CP/MAS NMR spectra are expected to be distinct among the lignin types present in different biomass materials (as discussed in detail in Section 3.4), which clearly contributes to the ineffectiveness of this method as well. In addition to the aforementioned points, the problem of non-uniform CP excitation profile may have a detrimental effect regarding the evaluation of the intensities of the aromatic signals, since these cover a wider chemical shift range in comparison with the methoxyl signal and the process of polarization transfer from  $^1\text{H}$  to  $^{13}\text{C}$  nuclei is in general more difficult to be uniformly achieved for the aromatic signals than for the aliphatic ones [42,43]. This is an additional aspect that makes the use of the methoxyl signal analysis preferable and it can explain why this method gives better results, at least for the group of different types of biomass materials studied in this work.

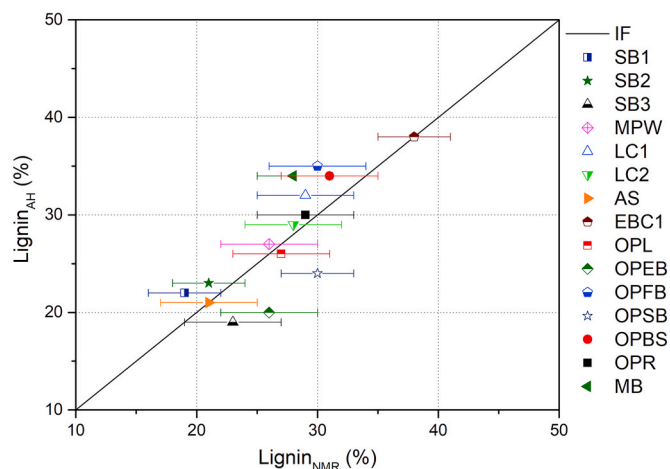


Fig. 2. Comparison between the lignin contents of several lignocellulosic materials obtained by the NMR-based method and by the acid hydrolysis (AH) method. The full line indicates the identity function (IF).

### 3.2. Study of chemically treated samples

The same NMR method was used for the analysis of chemically treated lignocellulosic materials (see Table 2). In these cases, the analysis of the lignin contents determined by NMR allowed the monitoring of the effects of the chemical processes employed. In the case of the SB-derived samples, for example, the NaOH treatments caused a progressive reduction of the lignin content, from 22% in the untreated sample to ca. 9% in the most severely treated samples. These trends were verified both using the proposed NMR approach and the much more laborious AH method, illustrating how useful solid-state NMR-based methods can be in cases where fast assessments of lignin contents are desirable in order to follow the effectiveness of chemical processing of lignocellulosic feedstock.

For the EG samples, the slightly higher content of p-hydroxyphenyl (around 5% w/w, relatively to the total lignin content) can cause an underestimation of the NMR-based lignin contents, as can be seen for the raw EG sample [15]. However, for the chemically treated EG samples, a good agreement between both methods was also observed, indicating the reduction of the lignin content with the sequence of chemical

treatments, which reinforces the potential of the NMR method in the study of NaOH-treated samples.

In the case of the EB-derived samples, on the other hand, the variations in the lignin contents caused by the chemical treatments occurred within the error ranges associated with the NMR method. Therefore, the proposed NMR approach was not useful in this case; for the accuracy level required in the case of these analyses, improvements in the method would be necessary, such as the use of a calibration curve constructed directly from the lignin extracted from the feedstock used in the chemical treatments.

Fig. 3 shows a comparison between the lignin contents obtained by AH and by the NMR-derived method for the chemically treated samples. These data can be divided into two groups with considerably different lignin contents. The group with lower lignin contents (below 15%) exhibited better agreement between the contents determined by NMR and by the AH method. On the other hand, the group with higher lignin contents (mostly above 20%) presented a larger difference between the values predicted by the two methods. As also shown in the same plot, these data can be further subdivided, considering the ratio between the intensity of the  $^{13}\text{C}$  NMR signal at 153 ppm and the sum of the intensities of the signals at 145 and 148 ppm (represented by the symbol  $r_{\text{SG}}$ ), which are all due to aromatic carbons in lignin [44]. The relative intensities of these signals are dependent on the chemical composition of the lignin present in each precursor and this affects the accuracy of the lignin contents determined by the NMR method, as it will be further discussed in Section 3.4.

### 3.3. Study of the “outlier samples” and solid-state $^{13}\text{C}$ NMR analyses of the AH lignin residues

For the samples EBC2, PKS1, PKS2, MKS1 and MKS2 the AH lignin contents were found to be substantially higher than the NMR-derived lignin contents and also noticeably high in comparison with values reported in the literature for typical lignocellulosic materials [24,29,41], which suggests that they may actually be overestimated for these samples.

In order to check this, the solid residues left after the chemical processing used in the AH method (which supposedly should represent the lignin and the ash content in the material) were also analysed by solid-state NMR. Fig. 4 shows the  $^{13}\text{C}$  CP/MAS NMR spectra obtained for the AH lignin residues (indicated by the suffix “AH”) of a number of samples, compared to the spectra recorded for the same respective raw lignocellulosic materials. The samples whose AH lignin residues were analysed by  $^{13}\text{C}$  CP/MAS NMR were the following: AS, EBC1, EBC2, MKS2, PKS1, PKS2, SB3, MB, OPL, OPEB; all these spectra are shown in the Supplementary Material and an asterisk was used in Table 1 to mark

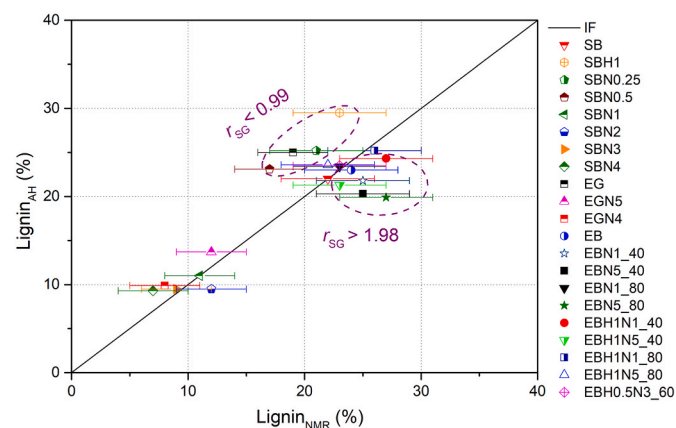


Fig. 3. Comparison between the lignin contents obtained by the NMR-based method and by the acid hydrolysis (AH) method for the chemically treated samples. The full line indicates the identity function (IF).

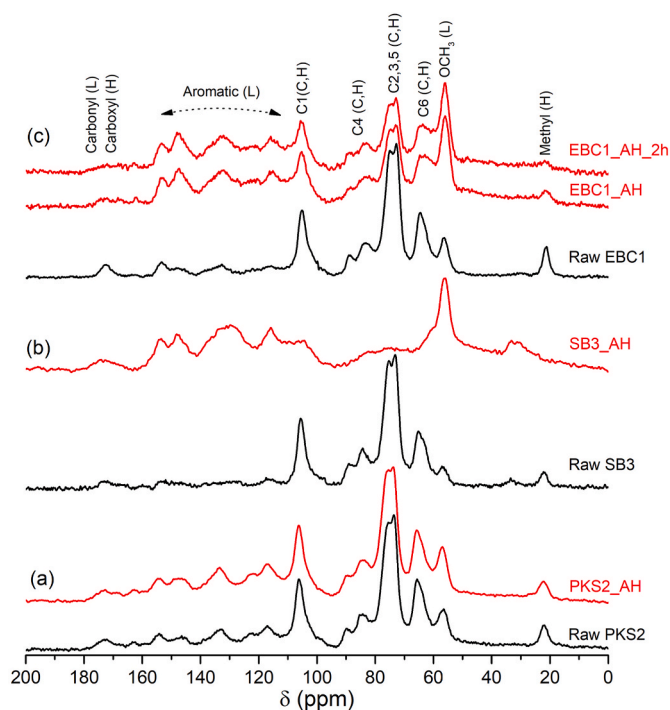


Fig. 4.  $^{13}\text{C}$  CP/MAS NMR spectra of the AH lignin residues (indicated by the suffix “AH”) compared to the spectra recorded for the respective raw materials for samples (a) PKS2, (b) SB3 and (c) EBC1. In the case of sample EBC1, the spectrum obtained for the residue of a more severe acid hydrolysis treatment (120 °C, 2 h) is also exhibited.

the samples for which carbohydrate signals were observed in the  $^{13}\text{C}$  CP/MAS NMR spectra.

As it is well known [31], the chemical reactions used in the procedure to determine the AH lignin aim to hydrolyse all the carbohydrates present in the sample, obtaining at the end a solid residue that is assumed (after subtraction of the ash and moisture contents) to represent the insoluble lignin content in the analysed material. However, the NMR spectra exhibited in Fig. 4 show that there are high amounts of carbohydrates in the residues obtained from PKS, for example; this is an evidence of the limited effectiveness of the acid attack to the carbohydrates present in some lignocellulosic precursors (notably those obtained from fruit kernel shells), which can be related to the morphology and chemical composition of each individual lignocellulosic matrix and constitutes a clear limitation on the reliability of AH-derived lignin contents [24,45].

A further test to solve this problem was performed in the case of the EBC1 sample, changing the reaction time in the acid hydrolysis reactor at 120 °C to 2 h, in an effort to try to dissolve completely the carbohydrates; however, the amount of carbohydrates in the residue was not reduced, as shown in Fig. 4c. On the other hand, it is interesting to observe in Table 1 that, in the case of the EBC1 sample, the relatively small amount of carbohydrates present in the residue (as seen in the spectra exhibited in Fig. 4c) did not cause a significant overestimation of the AH lignin contents, as there was a reasonable agreement with the NMR-derived values; the same was also true for the AS sample, where a small amount of carbohydrates was detected in the AH lignin residue, in spite of a good agreement between the NMR-derived and AH lignin contents.

On the other hand, the  $^{13}\text{C}$  CP/MAS NMR spectra recorded for the residue obtained for other precursors (such as SB, as also illustrated in Fig. 4b) were completely free of carbohydrate contributions. It is not surprising, therefore, the good agreement observed between the AH and the NMR-derived lignin contents in the case of SB and the huge discrepancy observed for PKS and for some of the other precursors

shown in Table 1. In these cases, the presence of significant amounts of carbohydrates in the AH residues indicates that the AH lignin contents are certainly overestimated; the NMR-derived method constitutes then a better alternative to deal with these materials, as also noted for other spectroscopic methods [40,46,47].

### 3.4. Influence of the type of lignin present in each material on the accuracy of the NMR-derived lignin contents

As discussed in Section 3.1, the choice of the intensity of the methoxyl peak in the  $^{13}\text{C}$  CP/MAS NMR spectra as an indicator of the lignin content in lignocellulosic materials may compromise the accuracy of the method when applied to a very diverse group of samples, since the amount of methoxyl groups can vary for the different phenolic units that can constitute the lignin structure. Therefore, a more detailed analysis of the  $^{13}\text{C}$  CP/MAS NMR spectra of the different lignocellulosic materials investigated in this work can help to understand the limits of application and to propose improvements in the method.

Based on an extensive compilation of previous reports in the literature (detailed in the Supplementary Material), the ratio of syringyl to guaiacyl units (S/G) in a lignocellulosic material can be inferred from an analysis of the chemical shift region in the  $^{13}\text{C}$  NMR spectra associated with the signals due to aromatic carbons in the lignin structure. Fig. 5 shows this expanded region of the  $^{13}\text{C}$  CP/MAS NMR spectra obtained for a group of samples analysed in this work. In general, it is possible to associate the signal near 153 ppm mainly with contributions due to syringyl units, whereas the signals at 145 and 148 ppm are mostly associated with guaiacyl units [48] and a distinct signal near 158 ppm is mostly due to carbon 4 of p-hydroxyphenyl units [23,49].

The values of the ratio (represented by the symbol  $r_{\text{SG}}$ ) between the

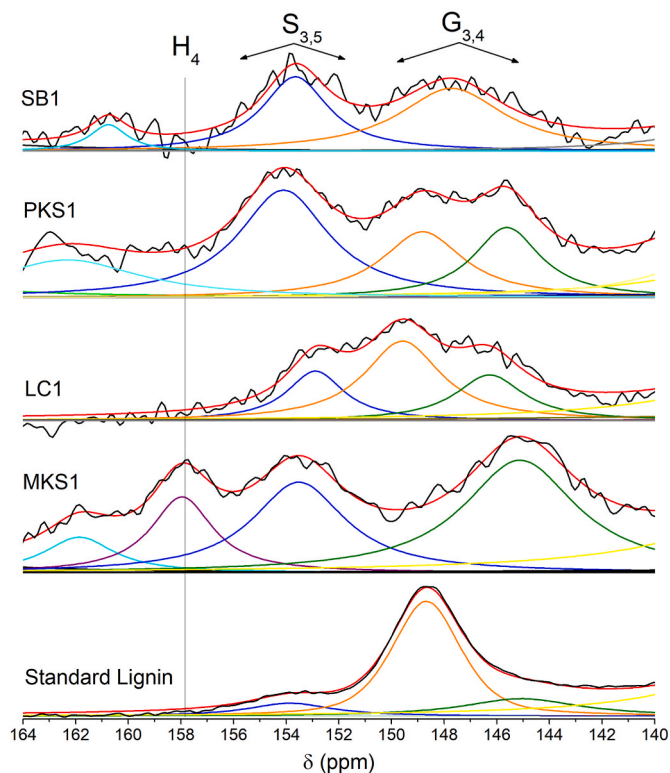


**Fig. 5.** Expanded view of the  $^{13}\text{C}$  CP/MAS NMR spectra obtained for selected lignocellulosic materials, showing the chemical shift region associated with the signals due to aromatic carbons in the lignin structure. The black line is the experimental spectrum, the red line is the fitted spectrum and the other lines correspond to the spectral components due to the indicated groups, as detailed in the text. (For interpretation of the references to colour in this figure legend, the reader is referred to the Web version of this article.)

intensity of the  $^{13}\text{C}$  NMR signal at 153 ppm and the sum of the intensities of the signals at 145 and 148 ppm, calculated from the  $^{13}\text{C}$  CP/MAS NMR spectra of all samples analysed in this work, are given in Tables 1 and 2. The same calculation was also carried out using quantitative  $^{13}\text{C}$  DP/MAS NMR spectra for a set of selected samples. A good agreement was observed in the comparison between the CP- and DP-derived values (given in the Supplementary Material), showing that the calculated  $r_{\text{SG}}$  values are indeed meaningful for inferring on the changes in the S/G ratio among the different lignocellulosic materials analysed in this work [44,50].

As it can be seen in Tables 1 and 2, the calculated  $r_{\text{SG}}$  values show large scattering among the different studied samples, which confirms that the samples are composed of different types of lignin. This fact can also be observed in Fig. 5, where the relevant spectral region in the  $^{13}\text{C}$  NMR spectra is compared for some of the studied lignocellulosic materials. It is important to note that the S/N ratio is low in this chemical shift range, which limits the accuracy of the spectral fittings (also shown in Fig. 5) and of the corresponding calculations of integrated intensities.

Even so, it is possible to observe from the analysis of the values given in Tables 1 and 2 that the  $r_{\text{SG}}$  values (which are expected to be roughly proportional to the S/G ratios) were lower than 0.5 for samples MPW, LC1 and LC2, which are typical softwoods; this finding is expected, since softwoods are typically richer in guaiacyl units [14,36]. At the same time, the  $r_{\text{SG}}$  values obtained for the EB sample were well above 1.0, indicating, as expected for hardwoods, a larger number of syringyl units [51]. Based on these trends, one can conclude that the lignocellulosic materials obtained from fruit endocarps, such as EBC, PKS, AS and MKS, are rich in syringyl units (similarly to hardwoods).

It is also worth noting that the standard lignin used for the construction of the calibration curve in the method described in this work (whose expanded  $^{13}\text{C}$  CP/MAS NMR spectrum is shown in Fig. 5) exhibited a small  $r_{\text{SG}}$  value (0.10), which indicates it is not rich in etherified syringyl units in comparison with guaiacyl units. The prevalence of guaiacyl units in this sample is thus supposed to contribute to minimize the errors in the NMR-derived lignin contents resulting from the variability of lignin chemical composition among the several lignocellulosic materials that were analysed, since a lignin sample rich in guaiacyl units is expected to present an intermediate average number of methoxyl groups in comparison to lignin samples rich in dimethoxylated (syringyl) or non-methoxylated (p-hydroxyphenyl) units.

Another important remark here is the presence of an intense signal at 158 ppm in the  $^{13}\text{C}$  CP/MAS NMR spectrum of sample MKS1 (Fig. 5), which is associated with p-hydroxyphenyl units [49], indicating the occurrence of a considerable amount of this phenolic unit in this sample. As p-hydroxyphenyl units do not have attached methoxyl groups, it is reasonable to assume that the lignin content predicted by the NMR method previously described (based on the intensity of the signal due to methoxyl groups) may be underestimated in the case of materials containing lignin rich in p-hydroxyphenyl units. This fact can also contribute to the large discrepancy observed between the NMR-derived and the Klason lignin contents in the case of the MKS samples (see Table 1).

As for the chemically treated samples, the subdivision presented in Fig. 3 suggests that the samples rich in syringyl units (i.e., with high  $r_{\text{SG}}$  values) had their lignin contents slightly overestimated by the NMR method, when compared to the AH method. Likewise, the samples with low  $r_{\text{SG}}$  values had their NMR-derived lignin contents slightly underestimated in comparison with the AH-derived values. This finding is an evidence of the influence of the chemical nature of the lignin present in each lignocellulosic material on the accuracy of the prediction of its lignin content by the NMR method here described.

However, it is important to point out that the lignin contents obtained by both methods were not in good agreement for just two (EBN5\_40 and EBN5\_80) of the ten samples with  $r_{\text{SG}}$  ratio higher than 1.98 presented in Table 2. For the eight other ones, the difference between the NMR- and AH-derived results was less than 1% for the samples

EB, EB1N1\_80, EB1N1N1\_80, EB1N5\_80 and EBH0.5N3\_60 and less than 3.2% for the others. These differences are smaller than the previously estimated uncertainty intervals, which shows that the errors associated with the NMR-derived method due to the structural chemical variation of lignin falls within the uncertainty margin of the result in most cases.

Summarizing, from a practical point of view, the proposed NMR method exhibits a number of advantages in comparison with the AH methods, such as: i) the possibility of recovering the samples after the analysis, since the NMR experiment is non-destructive; ii) the elimination of hazardous chemicals in the process; iii) the use of small amounts of sample (~30–40 mg are enough to fill a 4 mm NMR rotor); iv) fewer steps of sample manipulation and, lastly, v) reduced time to determine the lignin contents. Once the calibration curve has been constructed, the result of the lignin content can be obtained in a time considerably shorter (ca. 4 h) by NMR than the AH methods (ca.12.5 h), as described in Table S5 of the Supplementary Material. In most cases, good agreement is achieved between lignin contents obtained by NMR and AH and, in some cases, particularly in samples highly resistant to hydrolysis, NMR method gave more reliable results.

#### 4. Conclusions

<sup>13</sup>C CP/MAS NMR spectroscopy showed to be a useful tool to estimate the lignin contents of different biomass materials. Variation in the lignin chemical composition reduced the accuracy of the NMR-predicted values, but the observed errors remained within the estimated uncertainties, in most cases. The proposed method showed to be a good alternative to acid hydrolysis methods in cases where the complete hydrolysis of carbohydrates is not possible; it also constitutes an industrially applicable methodology for monitoring treatment processes of biomass materials, as it is fast, requires small sample amounts and does not involve hazardous chemicals.

#### Acknowledgements

The authors thank Prof. Eloi Silva (UFES) and the Fibria Company for providing the lignin sample. The technical support from CENPES/PETROBRAS and LabPetro/UFES and the financial support from the funding agencies Conselho Nacional de Desenvolvimento Científico e Tecnológico (CNPq) (projects #408001/2016-0 and #420031/2018-9), Coordenação de Aperfeiçoamento de Pessoal de Nível Superior (CAPES), Fundação Estadual de Amparo à Pesquisa do Estado do Espírito Santo (FAPES) (grant 73296872, TO 21/2016), Fundação de Amparo à Pesquisa do Estado de São Paulo (FAPESP) (project #2016/13602-7) and Financiadora de Estudos e Projetos (FINEP) are also greatly acknowledged.

#### Appendix A. Supplementary data

Supplementary data to this article can be found online at <https://doi.org/10.1016/j.biombioe.2020.105792>.

#### References

- [1] C. Somerville, H. Youngs, C. Taylor, S.C. Davis, S.P. Long, Feedstocks for lignocellulosic biofuels, *Science* 329 (2010) 790–792.
- [2] H.R. Amaral, D.F. Cipriano, M.S. Santos, M.A. Schettino, J.V.T. Ferreti, C. S. Meirelles, V.S. Pereira, A.G. Cunha, F.G. Emmerich, J.C.C. Freitas, Production of high-purity cellulose, cellulose acetate and cellulose-silica composite from babassu coconut shells, *Carbohydr. Polym.* 210 (2019) 127–134, <https://doi.org/10.1016/j.carbpol.2019.01.061>.
- [3] H. Wang, Y. Pu, A. Ragauskas, B. Yang, From lignin to valuable products—strategies, challenges, and prospects, *Bioresour. Technol.* 271 (2019) 449–461, <https://doi.org/10.1016/j.biortech.2018.09.072>.
- [4] A. Limayem, S.C. Ricke, Lignocellulosic biomass for bioethanol production: current perspectives, potential issues and future prospects, *Prog. Energy Combust. Sci.* 38 (2012) 449–467.
- [5] J. Goldemberg, The Brazilian biofuels industry, *Biotechnol. Biofuels* 1 (6) (2008) 1–7, <https://doi.org/10.1186/1754-6834-1-6>.
- [6] R. Singh, A. Shukla, S. Tiwari, M. Srivastava, A review on delignification of lignocellulosic biomass for enhancement of ethanol production potential, *Renew. Sustain. Energy Rev.* 32 (2014) 713–728, <https://doi.org/10.1016/j.rser.2014.01.051>.
- [7] Y. Gao, J. Xu, Y. Zhang, Q. Yu, Z. Yuan, Y. Liu, Effects of different pretreatment methods on chemical composition of sugarcane bagasse and enzymatic hydrolysis, *Bioresour. Technol.* 144 (2013) 396–400, <https://doi.org/10.1016/j.biortech.2013.06.036>.
- [8] G. Tzoumis, *Science and Technology of Wood: Structure, Properties, Utilization*, first ed., Chapman & Hall, New York, 1991.
- [9] P. Albersheim, A. Darvill, K. Roberts, R. Sederoff, A. Staehelin, *Plant Cell Walls*, first ed., Garland Science, New York, 2010.
- [10] R.J. Moon, A. Martini, J. Nairn, J. Simonsen, J. Youngblood, Cellulose nanomaterials review: structure, properties and nanocomposites, *Chem. Soc. Rev.* 40 (2011) 3941–3994, <https://doi.org/10.1039/c0cs00108b>.
- [11] H.W. Heldt, B. Piechulla, F. Heldt, *Plant Biochemistry*, third ed., Academic Press, 2005 <https://doi.org/10.1016/B978-0-12-088391-2.X5000-7>.
- [12] R. Whetten, R. Sederoff, Lignin biosynthesis, *Plant Cell* 7 (1995) 1001–1013, <https://doi.org/10.1105/tpc.7.7.1001>.
- [13] Y. Gnanou, M. Fontanille, *Organic and Physical Chemistry of Polymers*, John Wiley & Sons, 2008.
- [14] L.H.S. Zobiolo, W.D. dos Santos, E. Bonini, O. Ferrarese-Filho, R.J. Kremer, R.S. de Oliveira Jr., J. Constantin, Lignin: from nature to industry, in: R.J. Paterson (Ed.), *Lignin Prop. Appl. Biotechnol. Bioenergy, Nova Science*, 2012, pp. 419–435.
- [15] X. Tian, Z. Fang, R.L. Smith, Z. Wu, M. Liu, Properties, chemical characteristics and application of lignin and its derivatives, in: Z. Fang, R.L. Smith (Eds.), *Biofuels Chem. From Lignin*, Springer, Singapore, 2016, pp. 3–34, [https://doi.org/10.1007/978-981-10-1965-4\\_1](https://doi.org/10.1007/978-981-10-1965-4_1).
- [16] D. Kai, M.J. Tan, P.L. Chee, Y.K. Chua, Y.L. Yap, X.J. Loh, Towards lignin-based functional materials in a sustainable world, *Green Chem.* 18 (2016) 1175–1200, <https://doi.org/10.1039/c5gc02616d>.
- [17] K. Hofsetz, M.A. Silva, Brazilian sugarcane bagasse: energy and non-energy consumption, *Biomass Bioenergy* 46 (2012) 564–573, <https://doi.org/10.1016/j.biombioe.2012.06.038>.
- [18] S. Nanda, J. Mohammad, S.N. Reddy, J.A. Kozinski, A.K. Dalai, Pathways of lignocellulosic biomass conversion to renewable fuels, *Biomass Convers. Biorefinery.* 4 (2014) 157–191, <https://doi.org/10.1007/s13399-013-0097-z>.
- [19] C. Rezende, M. de Lima, P. Maziero, E. deAzevedo, W. Garcia, I. Polikarpov, Chemical and morphological characterization of sugarcane bagasse submitted to a delignification process for enhanced enzymatic digestibility, *Biotechnol. Biofuels* 4 (2011) 54, <https://doi.org/10.1186/1754-6834-4-54>.
- [20] Z. Qin, X. De Wang, H.M. Liu, D.M. Wang, G.Y. Qin, Structural characterization of Chinese quince fruit lignin pretreated with enzymatic hydrolysis, *Bioresour. Technol.* 262 (2018) 212–220, <https://doi.org/10.1016/j.biortech.2018.04.072>.
- [21] B.R. Hames, S.R. Thomas, A.D. Sluiter, C.J. Roth, D.W. Templeton, Rapid biomass analysis, in: B.H. Davison, J.W. Lee, M. Finkelstein, J.D. McMillan (Eds.), *Biotechnol. Fuels Chem. Twenty-Fourth Symp.*, Humana Press, Totowa, NJ, 2003, pp. 5–16, [https://doi.org/10.1007/978-1-4612-0057-4\\_1](https://doi.org/10.1007/978-1-4612-0057-4_1).
- [22] J.C.C. Freitas, T.J. Bonagamba, F.G. Emmerich, Investigation of biomass- and polymer-based carbon materials using <sup>13</sup>C high-resolution solid-state NMR, *Carbon N. Y.* 39 (2001) 535–545, [https://doi.org/10.1016/S0008-6223\(00\)00169-X](https://doi.org/10.1016/S0008-6223(00)00169-X).
- [23] F.A. Perras, H. Luo, X. Zhang, N.S. Mosier, M. Pruski, M.M. Abu-Omar, Atomic-level structure characterization of biomass pre- and post-lignin treatment by dynamic nuclear polarization-enhanced solid-state NMR, *J. Phys. Chem.* 121 (2017) 623–630, <https://doi.org/10.1021/acs.jpca.6b11121>.
- [24] S.H. Ghaffar, M. Fan, Structural analysis for lignin characteristics in biomass straw, *Biomass Bioenergy* 57 (2013) 264–279, <https://doi.org/10.1016/j.biombioe.2013.07.015>.
- [25] J. Freitas, A. Cunha, F. Emmerich, Solid-state nuclear magnetic resonance methods applied to the study of carbon materials, in: L. Radovic (Ed.), *Chem. Physics Carbon*, CRC Press, Boca Raton, 2012, pp. 85–170, <https://doi.org/10.1201/b12960-3>.
- [26] L. Fu, S.A. McCallum, J. Miao, C. Hart, G.J. Tudryn, F. Zhang, R.J. Linhardt, Rapid and accurate determination of the lignin content of lignocellulosic biomass by solid-state NMR, *Fuel* 141 (2015) 39–45, <https://doi.org/10.1016/j.fuel.2014.10.039>.
- [27] C. Sievers, T. Marzalletti, T.J.C. Hoskins, M.B. Valenzuela Olarte, P.K. Agrawal, C. W. Jones, Quantitative solid state NMR analysis of residues from acid hydrolysis of loblolly pine wood, *Bioresour. Technol.* 100 (2009) 4758–4765, <https://doi.org/10.1016/j.biortech.2008.11.060>.
- [28] J.F. Haw, G.E. Maciel, H.A. Schroeder, Carbon - 13 nuclear magnetic resonance spectrometric study of wood and wood pulping with cross polarization and magic-angle spinning, *Anal. Chem.* 56 (1984) 1323–1329, <https://doi.org/10.1021/pr200800w>.
- [29] X. Gao, D.D. Laskar, J. Zeng, G.L. Helms, S. Chen, A <sup>13</sup>C CP/MAS-based nondegradative method for lignin content analysis, *ACS Sustain. Chem. Eng.* 3 (2015) 153–162, <https://doi.org/10.1021/sc500628s>.
- [30] R. Hatfield, R.S. Fukushima, Can lignin be accurately measured? *Crop Sci.* 45 (2005) 832–839, <https://doi.org/10.2135/cropsci2004.0238>.
- [31] Tappi, T222 Om-02 Lignin in Wood and Pulp, TAPPI Test Methods, vols. 1–7, 2006 accessed, <https://www.tappi.org/content/SARG/T222.pdf>. (Accessed 23 January 2019).
- [32] S.A. Nascimento, C.A. Rezende, Combined approaches to obtain cellulose nanocrystals, nanofibrils and fermentable sugars from elephant grass, *Carbohydr. Polym.* 180 (2018) 38–45, <https://doi.org/10.1016/j.carbpol.2017.09.099>.

- [33] D.G. Cory, W.M. Ritchey, Suppression of signals from the probe in bloch decay spectra, *J. Magn. Reson.* 80 (1988) 128–132, [https://doi.org/10.1016/0022-2364\(88\)90064-9](https://doi.org/10.1016/0022-2364(88)90064-9).
- [34] ACD/NMR Processor Academic Edition (n.d.), [www.acdlabs.com](http://www.acdlabs.com). (Accessed 29 May 2015), [www.acdlabs.com](http://www.acdlabs.com).
- [35] J.C. del Río, A.G. Lino, J.L. Colodette, C.F. Lima, A. Gutiérrez, Á.T. Martínez, F. Lu, J. Ralph, J. Rencoret, Differences in the chemical structure of the lignins from sugarcane bagasse and straw, *Biomass Bioenergy* 81 (2015) 322–338, <https://doi.org/10.1016/j.biombioe.2015.07.006>.
- [36] R. Vanholme, B. Demedts, K. Morreel, J. Ralph, W. Boerjan, Lignin biosynthesis and structure, *Plant Physiol.* 153 (2010) 895–905, <https://doi.org/10.1104/pp.110.155119>.
- [37] W. Kolodziejski, J.S. Frye, G.E. Maciel, Carbon-13 nuclear magnetic resonance spectrometry with cross polarization and magic-angle spinning for analysis of lodgepole pine wood, *Anal. Chem.* 54 (8) (1982) 1419–1424, <https://doi.org/10.1021/ac00245a035>.
- [38] J. Ralph, K. Lundquist, G. Brunow, F. Lu, H. Kim, P.F. Schatz, J.M. Marita, R. D. Hatfield, S.A. Ralph, J.H. Christensen, W. Boerjan, Lignins: natural polymers from oxidative coupling of 4-hydroxyphenyl-propanoids, *Phytochemistry Rev.* 3 (2004) 29–60, <https://doi.org/10.1023/B:PHYT.0000047809.65444.a4>.
- [39] S.Y. Lin, C.W. Dence, *Methods in Lignin Chemistry*, Springer-Verlag, Berlin, 1992, <https://doi.org/10.1007/978-3-642-74065-7>.
- [40] M.A. Sanderson, F. Agblevor, M. Collins, D.K. Johnson, Compositional analysis of biomass feedstocks by near infrared reflectance spectroscopy, *Biomass Bioenergy* 11 (1996) 365–370, [https://doi.org/10.1016/S0961-9534\(96\)00039-6](https://doi.org/10.1016/S0961-9534(96)00039-6).
- [41] R.S. Fukushima, R.D. Hatfield, Comparison of the acetyl bromide spectrophotometric method with other analytical lignin methods for determining lignin concentration in forage samples, *J. Agric. Food Chem.* 52 (2004) 3713–3720, <https://doi.org/10.1021/jf035497l>.
- [42] R.J. Smernik, J.M. Oades, The use of spin counting for determining quantitation in solid state <sup>13</sup>C NMR spectra of natural organic matter 2. HF-treated soil fractions, *Geoderma* 96 (2000) 159–171, [https://doi.org/10.1016/S0016-7061\(00\)00007-0](https://doi.org/10.1016/S0016-7061(00)00007-0).
- [43] G.R. Hatfield, G.E. Maciel, O. Erbaturo, G. Erbaturo, Qualitative and quantitative analysis of solid lignin samples by carbon-13 nuclear magnetic resonance spectrometry, *Anal. Chem.* 59 (1987) 172–179, <https://doi.org/10.1021/ac00128a036>.
- [44] H. Wikberg, S.L. Maunu, Characterisation of thermally modified hard- and softwoods by <sup>13</sup>C CPMAS NMR, *Carbohydr. Polym.* 58 (2004) 461–466, <https://doi.org/10.1016/j.carbpol.2004.08.008>.
- [45] R.D. Hatfield, H.-J.G. Jung, J. Ralph, D.R. Buxton, P.J. Weimer, A comparison of the insoluble residues produced by the Klason lignin and acid detergent lignin procedures, *J. Sci. Food Agric.* 65 (1994) 51–58, <https://doi.org/10.1002/jsfa.2740650109>.
- [46] F.C. Moreira-Vilar, R.D.C. Siqueira-Soares, A. Finger-Teixeira, D.M. De Oliveira, A. P. Ferro, G.J. Da Rocha, M.D.L.L. Ferrarese, W.D. Dos Santos, O. Ferrarese-Filho, The acetyl bromide method is faster, simpler and presents best recovery of lignin in different herbaceous tissues than klason and thioglycolic acid methods, *PLoS One* 9 (2014), e110000, <https://doi.org/10.1371/journal.pone.0110000>.
- [47] S.S. Kelley, R.M. Rowell, M. Davis, C.K. Jurich, R. Ibach, Rapid analysis of the chemical composition of agricultural fibers using near infrared spectroscopy and pyrolysis molecular beam mass spectrometry, *Biomass Bioenergy* 27 (2004) 77–88, <https://doi.org/10.1016/j.biombioe.2003.11.005>.
- [48] W.F. Manders, Solid-state <sup>13</sup>C NMR determination of syringyl/guaiacyl ratio in hardwoods, *Holzforchung* 41 (1987) 13–18.
- [49] H.-D. Lüdemann, H. Nimz, Carbon-13 nuclear magnetic resonance spectra of lignins, *Biochem. Biophys. Res. Commun.* 52 (1973) 1162–1169, [https://doi.org/10.1016/0006-291X\(73\)90622-0](https://doi.org/10.1016/0006-291X(73)90622-0).
- [50] A.T. Martínez, G. Almendros, F.J. González-Vila, R. Fründ, Solid-state spectroscopic analysis of lignins from several Austral hardwoods, *Solid State Nucl. Magn. Reson.* 15 (1999) 41–48, [https://doi.org/10.1016/S0926-2040\(99\)00045-4](https://doi.org/10.1016/S0926-2040(99)00045-4).
- [51] I. Kögel-Knabner, The macromolecular organic composition of plant and microbial residues as inputs to soil organic matter, *Soil Biol. Biochem.* 34 (2002) 139–162, <https://doi.org/10.1016/j.soilbio.2016.08.011>.